Optics & Laser Technology 42 (2010) 180–185

Contents lists available at ScienceDirect

Optics & Laser Technology

journal homepage: www.elsevier.com/locate/optlastec

Cosine bend-linear waveguide digital optical switch with parabolic heater

Ian Yulianti *, Abu Sahmah Mohd. Supa'at, Sevia M. Idrus, Abdulaziz M. Al-hetar

Photonics Technology Centre, Faculty of Electrical Engineering, Universiti Teknologi Malaysia, 81310 Johor, Malaysia

ARTICLE INFO

Article history:
Received 24 November 2008
Received in revised form
11 June 2009
Accepted 12 June 2009
Available online 10 July 2009

Keywords:
Digital optical switch
Thermo-optic switch
Cosine S-bend

ABSTRACT

A new digital optical switch (DOS) with large branching angle and short device length that exhibits low crosstalk and low power consumption is demonstrated. The Y-branch shape was optimized by introducing constant effective refractive index difference between branches (ΔN_{eff}) along the propagation direction through beam propagation method (BPM) scheme. To provide decreasing local branching angle that results in the improvement of the crosstalk, two modified cosine bend was introduced to form the Y-branch. The modified cosine branch was then connected to a linear branch. The heater electrode was optimized so that the temperature fields induce a constant ΔN_{eff} to satisfy initial assumption in designing the Y-branch shape. With branching angle of 0.299° and device length of only 5 mm, the simulation shows that the device could exhibits crosstalk of −33 dB at calculated required power of only 26 mW.

1. Introduction

The optical switches characteristic play an important role in optical networks as it determines the optical networks performance. The optical switch with low crosstalk (CT), low loss, low power consumption as well as wavelength and polarization insensitivity is preferable in optical networks. The mode sorting effect-based optical switch, well known as digital optical switch (DOS), is attractive to perform switch function in optical networks due to its robustness to variations in critical parameters such as electrical power applied, polarization, wavelength, temperature and even device geometrical variations [1]. In principle, a signal switching from the input port to one of the output branch in DOS is a result of refractive index difference between branches (Δn) in a Y-branch. The light launched at the input port is guided to the branch with the higher refractive index. The change in refractive index may be induced by applying voltage (electro-optic effect) or heat (thermo-optic effect) to the selected selections. The DOS is useful in the sense that additional applied power, beyond the switching power, does not degrade the crosstalk.

An electro-optic DOS-based on LiNbO3 has high performance such as able to change its state extremely rapid (less than nanosecond) and reliable [2]. However, it has high insertion loss, possible polarization dependence and high fabrication cost. Thermo-optic switches are generally small in size and the optical parameters, such as crosstalk and insertion loss, are acceptable for many application. Due to the highly efficient thermo-optic index modulation and low operating power, polymer waveguide based thermo-optic devices is currently intensively developed [3–5].

Linear Y-branch with very small branching angle is commonly used in DOS to minimize mode coupling between the local system modes. This small branching angle leads to long interaction lengths [6] thus it is not sufficient for large switching matrix that requires cascading many stages of switches. Furthermore, small branching angle causes difficulty in fabrication process. Conventional linear DOS also has the drawback of having high switching power. Polymeric thermo-optic DOS with large branching angle has been developed earlier [7], however, the device still consume high dissipated power. In this paper, we present a new DOS design in which the Y-branch is formed by modified cosine bend connected to linear waveguide and the heater is parabolic in shape. The combination of modified cosine bend branch and parabolic heater enhances the branching angle, improves the device compactness while exhibits relatively low crosstalk value at low electric power.

2. Y-junction shape optimization

The switch function depends strongly on the coupling behavior between the two waveguides along the propagation direction. The mode coupling in Y-branch is proportional to the local full branch angle, as defined by [8]

$$\gamma = 2\frac{C_{ij}}{\Delta\beta_{ij}}\tan\left(\frac{\theta}{2}\right) \quad (1)$$

where γ determines mode coupling between the normal modes. $\Delta\beta_{ij}$ and C_{ij} are normal mode asynchronism and coupling constant,

* Corresponding author. Tel.: +60 75536202; fax: +60 75566272.
E-mail address: ianyulianti@yahoo.com (I. Yulianti).

0030-3992/$ - see front matter © 2009 Elsevier Ltd. All rights reserved.
doi:10.1016/j.optlastec.2009.06.003

respectively, whereas θ is the full branch angle. The peak of γ decreases and occurs in a smaller waveguide gap as the index difference between waveguides increases [9]. The γ becomes constant and the level of peak at small index difference is smaller if the local full branch angle is decreased at a large waveguide gap, thus the crosstalk could be reduced [9].

A Y-branch with decreasing local branching angle could be developed from two short cosine S-bend waveguides. However, previous study [10] shows that the cosine S-bend Y-branch does not significantly reduce the crosstalk. To further improve the crosstalk performance, we proposed the modified cosine bend that is connected to linear branch (Fig. 1). The lateral position of the modified cosine bend is defined by

$$x(z) = A\left(1 - \cos\left(\frac{2\pi}{3L}z\right)\right) \quad (2)$$

As implied in (2), the modified cosine bend is the cosine S-bend in which the length is one-third of the cosine function period. The modified cosine bend was also chosen to provide smooth connection to the input waveguide that leads to the reduction of the connection loss.

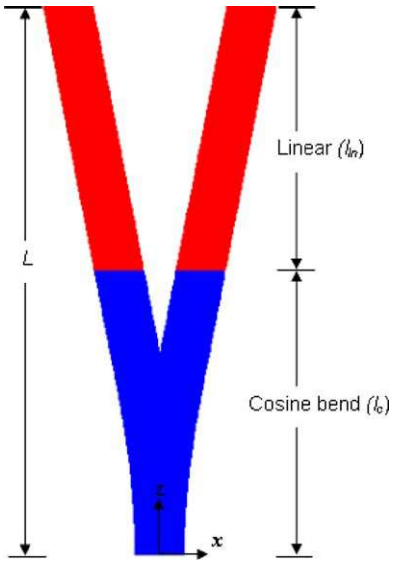

Fig. 1. Top view of the proposed Y-junction structure.

The crosstalk performance of the modified cosine bend–linear hybrid branch was investigated using beam propagation method (BPM) by introducing constant refractive index difference (Δn) between branches along propagation distance which leads to the difference in effective refractive index (ΔN_{eff}) as proposed by Moosburger et al. [11] and Hauffe [12]. The waveguide was determined to be buried square waveguide (BSC) with a $7 \times 7\,\mu m^2$ cross section. The BSC waveguides have the advantage of good fiber-to-waveguide coupling and little polarization dependency than rectangular waveguide. To avoid mode attenuation to the heater, the upper cladding thickness was determined to be 10 μm. Meanwhile, upper lower cladding was determined to be 20 μm. The material was assumed to be photo-active UV curable fluorinated resins based on acrylate with refractive index of core and cladding are 1.464 and 1.459, respectively. The thermo-optic coefficient (TOC) is -1.7×10^{-4}/K and the thermal conductivity is 0.17 W/m K. The simulation for three different opening angle of 0.299°, 0.288° and 0.268° has been done previously [13] by varying the length of modified cosine bend while maintaining the total length (L) which was determined to be 5 mm on TE mode at operating wavelength of 1.55 μm. The cosine bend junction length (l_c) was determined to be 2.6, 2.7 and 2.9 mm, respectively, and the amplitude A was determined to be 3.25 μm. The simulation result shows that the crosstalk for l_c of 2.7 and 2.9 mm oscillate with increasing effective refractive index difference and less oscillates for l_c of 2.6 mm.

If l_c is kept constant at 2.6 mm and alternatively the linear length (l_{ln}) is increased consecutively from $l_{ln} = 2.4$, 3.4 and 4.4 mm and thus the L is 5, 6 and 7 mm, respectively, the crosstalk performance does not significantly change as shown in Fig. 2(a). It can be concluded that at L of 5 mm, the first order of local mode has been fully transferred to the unheated branch and it is not necessary to lengthen the linear branch.

As a comparison, a simulation has also been done for a conventional Y-branch having the same opening angle. As can be seen in Fig. 2(b), to achieve −34 dB of crosstalk, the proposed Y-branch needs ΔN_{eff} of around 0.00128. Meanwhile, the conventional linear Y-branch needs higher index modulation which is

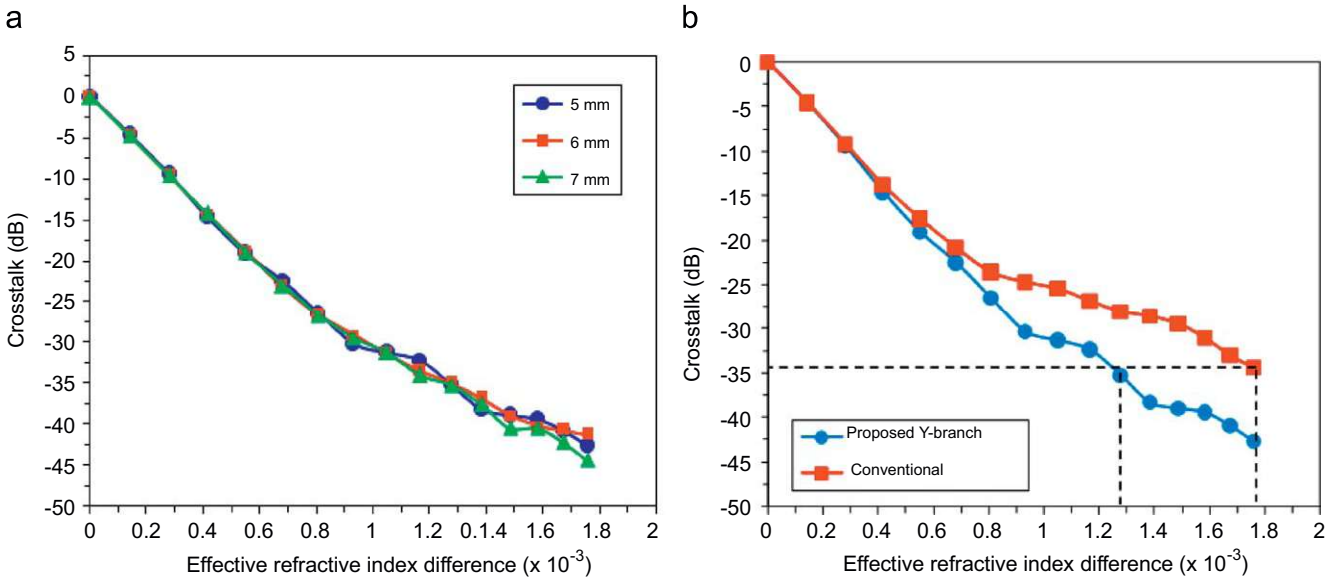

Fig. 2. Crosstalk performance of various linear branch lengths at a constant opening angle (a) and comparison of the performance of the proposed Y-branch to that of the conventional Y-branch (b).

nearly 0.0018. Thus, the proposed Y-branch requires almost 28% lower switching power than the conventional Y-branch.

3. Heater optimization

To satisfy initial condition applied in designing Y-branch shape, the heater was designed so that the ΔN_{eff} induced by the heater is constant along the propagation direction. This can be achieved by analyze the temperature distribution induce by the heater in the Y-branch. The temperature distribution is used to determine the spatial perturbation of the refractive index in the structure through the thermo-optic coefficient, dn/dT of the material. This perturbation is then incorporated into scalar Helmholtz wave equation of TE mode to determine the new effective refractive index for each branch. The propagation constants (β) of the branches are calculated by considering that the branches are perfectly separated such that there is no coupling between channel modes. The heater lateral position is optimized by determining the ΔN_{eff} (for a constant width) for various heater lateral positions in x direction (various d in Fig. 3) at certain cross-sections point (certain z). This procedure is repeated for a number of cross sections that is done by varying the waveguide gap, g in Fig. 3, which means a number of z value, varying from the arms separation point until the end of the Y-branch. The heater shape is then defined by the heater lateral position (x) as function of propagation distance (z) that exhibits the same value for ΔN_{eff} in all cross sections.

To evaluate the temperature distribution in the waveguide, the equation to be solved is the heat transfer equation in transient condition with constant thermal conductivity

$$k\nabla^2 T + Q(x,y,z,t) = \rho c_p \frac{\partial T}{\partial t} \tag{3}$$

where ρ is the material density, c_p the specific heat, k the thermal conductivity and $Q(x,y,z,t)$ the heat generation rate per unit volume. For steady-state heat conduction, Eq. (2) can be deduced to

$$k\nabla^2 T + Q(x,y,z,t) = 0 \tag{4}$$

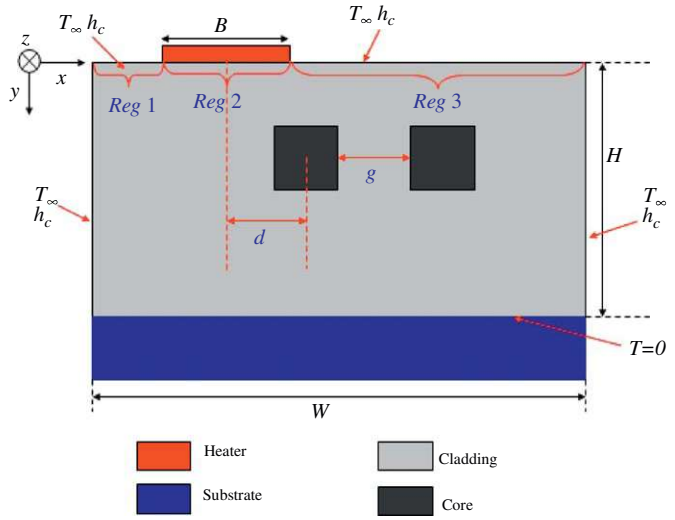

Fig. 3. Boundary condition illustration of Y-branch cross section with a heater electrode at certain point in the z-direction.

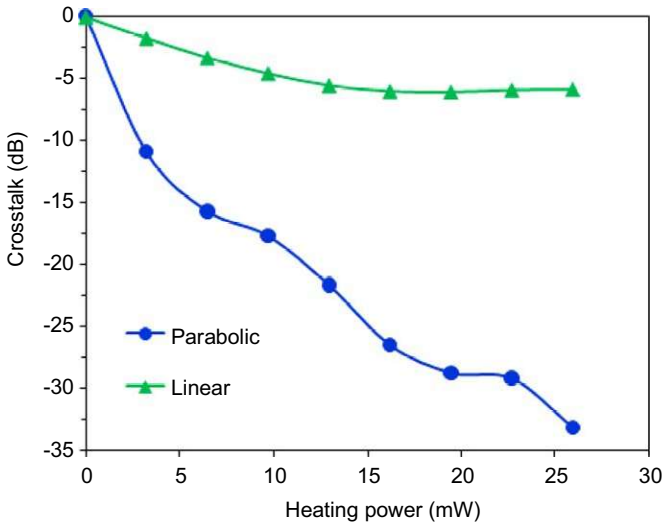

Fig. 5. Crosstalk response of cosine bend-linear Y-branch to heating power.

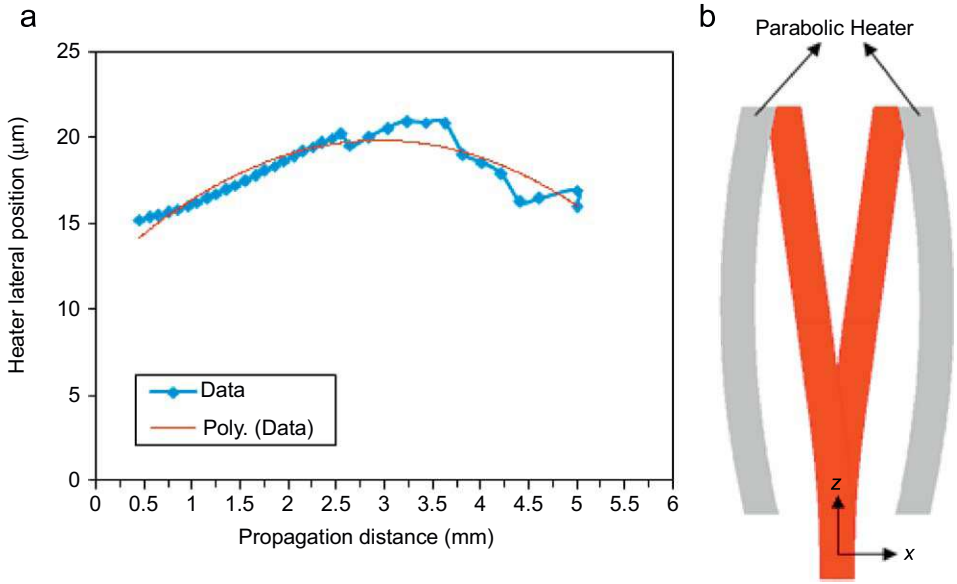

Fig. 4. Heater lateral position (x) as function of propagation distance (z) which induces constant ΔN_{eff} along the propagation distance (a) and top view of heater layout in the modified Y-branch (b).

For structure in which the length is much longer than the width such as the heater electrode in DOS, the thermal analysis can be represented by two-dimensional analysis. Therefore, the governing equation for steady-state heat conduction is then defined by

$$k\left(\frac{\partial^2 T(x,y)}{\partial x^2}+\frac{\partial^2 T(x,y)}{\partial^2 y^2}\right)+Q(x,y,z,t)=0 \quad (5)$$

Since the material used for core and cladding is the same material, which is acrylate polymer, the thermal conductivity of core and cladding material are assume to be identical. Eq. (5) is solved by employing finite difference method (FDM) after applying some boundary conditions as follows:

- for left-side surface:

$$-k\frac{\partial T}{\partial x}\Big|_{x=0}=h_c(T|_{x=0}-T_\infty) \quad (6)$$

- for right-side surface:

$$-k\frac{\partial T}{\partial x}\Big|_{x=W}=h_c(T|_{x=W}-T_\infty) \quad (7)$$

where h_c is the heat transfer coefficient of air and T_∞ the air upstream temperature.

At the top surface, the boundary condition is specified in three regions as shown in Fig. 3

- Region 1and region 3
  The surface is subjected to the convection.

$$-k\frac{\partial T}{\partial y}\Big|_{y=0}=h_c(T|_{y=0}-T_\infty) \quad (8)$$

- Region 2
  The surface is subjected to the heat flux originated from the heater electrode. The boundary condition applied in this

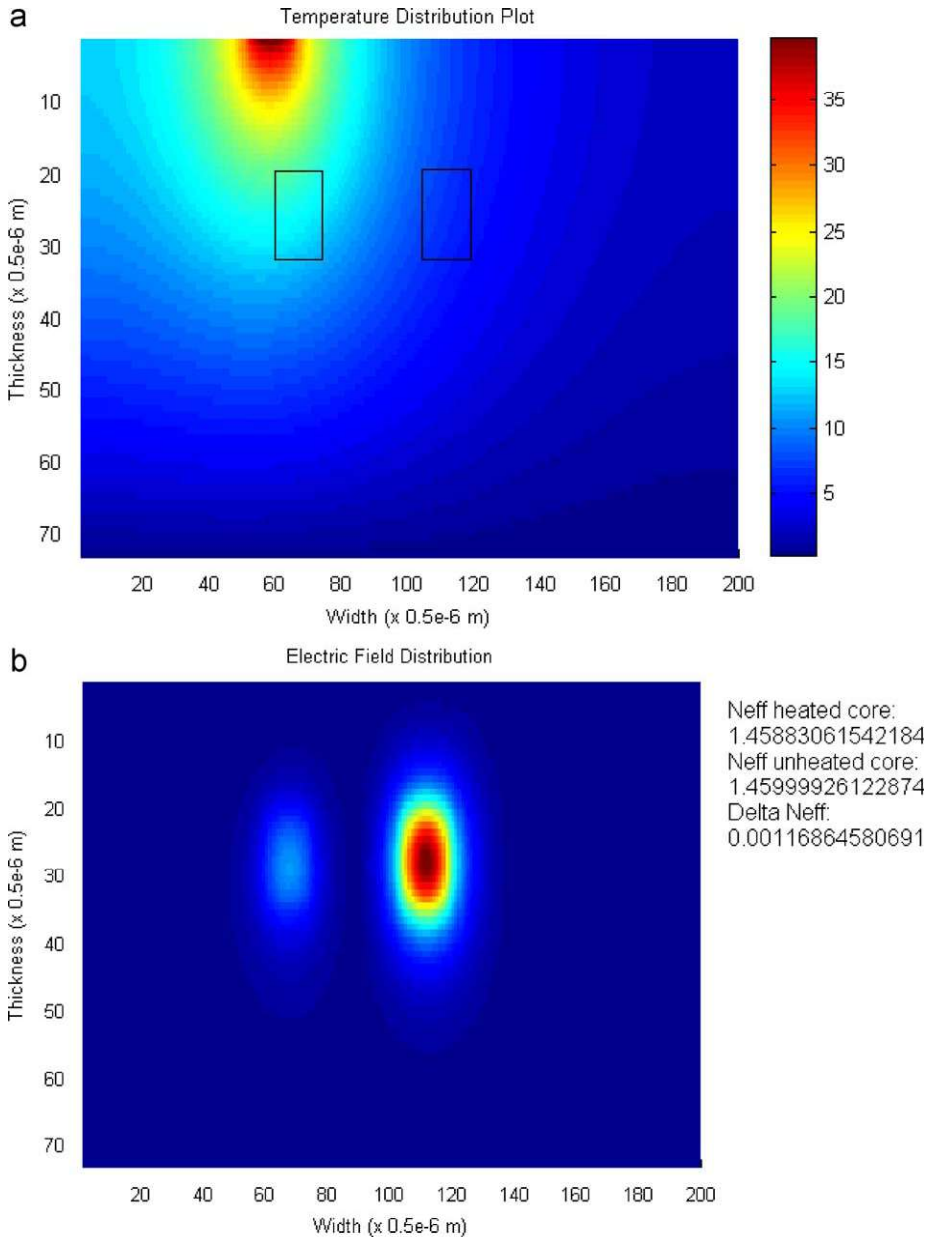

Fig. 6. The temperature distribution (a) and electric field distribution (b) induced by the heater with applied power of 26 mW.

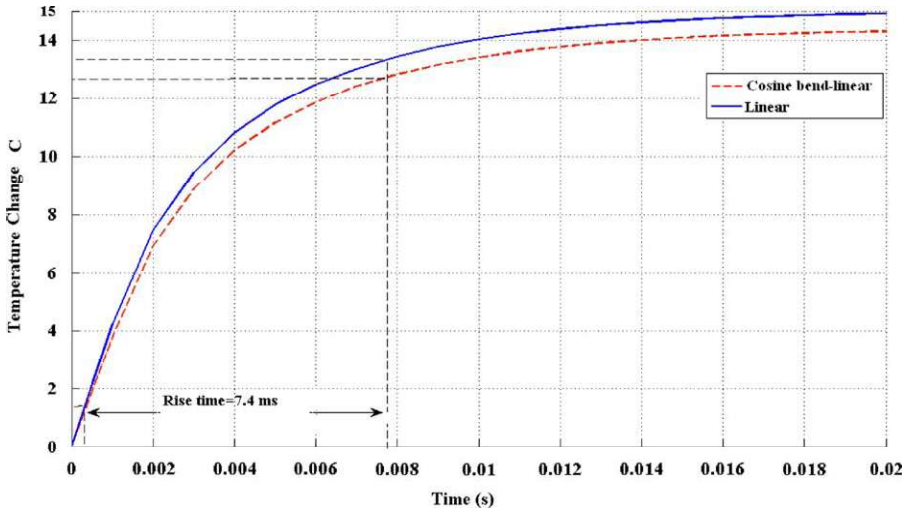

Fig. 7. Rise time for conventional linear DOS and cosine bend-linear DOS.

region is the *Neumann boundary condition* with the constant heat flux.

$$-k\left.\frac{\partial T}{\partial y}\right|_{y=0} = \frac{P}{BL_h} \tag{9}$$

where P is the applied power, B the heater width and L_h the heater length.

At the bottom surface, the silicon substrate is considered as a perfect heat sink due to its high thermal conductivity. The temperature assumed to be 0 °C [14].

$$T|_{y=H} = 0\,^{\circ}\mathrm{C} \tag{10}$$

The equations derived above are solved by using numerical method. The numerical method applied in this work is FDM by employing successive over relaxation (SOR) as an iterative method to enhance the rate of convergence [15]. In this work, the source code for thermal analysis FDM has been integrated with the FDM for Helmholtz wave equation solution so that the ΔN_{eff} induced by the heater can be directly determined.

The heater lateral position (x) as function of propagation distance (z) which induces constant ΔN_{eff} along the propagation distance for modified cosine bend–linear hybrid branch structure is depicted in Fig. 4(a). The simulation was done for heater width of 7 μm and z starts from 450 μm where the cosine bend arms begin to be shifted until the end of the branch which is 5000 μm. To obtain smooth curve of the heater position, the graph was fitted by a second order polynomial as defined by

$$x(z) = -0.9 \times 10^{-6} z^2 + 0.005z + 13.5(\mu\mathrm{m}) \tag{11}$$

The heater electrode shape defined by (11) is parabolic heater as (11) is a parabolic equation. The heater will be in the closest distance to the waveguide at the end of the branch. Eq. (11) is valid for heater in the positive x direction (right branch) as shown in Fig. 4(b). For left branch heater, the equation could be simply obtained by changing all the sign in (11).

The simulation of the thermal field induced by the parabolic heater effect to the light propagation in the modified cosine bend–linear hybrid branch structure was then carried out using commercial software BeamPropTM for validation purpose. For comparison, the simulation was also done for conventional linear heater. As shown in Fig. 5, it is clear that the parabolic heater performs the switching function more efficiently compare to the linear heater. Crosstalk of −33 dB could be achieved at calculated heating power of 26 mW, meanwhile the linear heater will only exhibits −5 dB of crosstalk. The increased temperature resulted from this heating power at the heater-cladding top surface interface and at the center of the heated core at the end of the branch is around 40 °C and around 14 °C, respectively, as shown in Fig. 6. For conventional linear heater, the temperature increased at the center of the heated core is around 15 °C. Due to the good thermal stability of polymer materials, this temperature change will not degrade the material performance. The stress induced by temperature change of 40 °C is 8 MPa which is much below the typical tensile strengths at yield for engineering polymers (50 MPa) [16]. Based on numerical solution for the thermal analysis integrated with the modal analysis, this temperature change will induce ΔN_{eff} of 0.0011658 as shown in Fig. 6. This result agrees with the simulation done by directly changing the refractive index of the branch as previously shown in Fig. 3 in which the effective refractive index change of around 0.001 will exhibits crosstalk value of −32 dB. Thus, the parabolic heater could induce the constant ΔN_{eff} that leads to the improvement of the crosstalk of the DOS.

The rise time response of the cosine bend-linear DOS and the conventional linear DOS has also been performed. As shown in Fig. 7, the rise time for cosine bend-linear DOS is equal to that of conventional DOS which is 7.4 ms. The equality of the rise time value of both devices is reasonable since the rise time depend on the heater to substrate distance, thermal conductivity of the materials and the waveguide structure (such as groove and trench) [5,17], meanwhile the heater geometry and Y-junction geometry do not contribute to the rise time value. The rise time could be further improved by re-optimizing the upper cladding and lower cladding thicknesses.

4. Conclusions

We have demonstrated the DOS constructed by modified cosine bend and linear waveguide as a Y-junction and by parabolic heater to induce thermal fields. Due to its larger branching angle, our design could overcome the fabrication problem. The heater shape which is determined to be parabolic could efficiently induce the temperature distribution to significantly improve the crosstalk. The device length is relatively short compare to that of the DOS currently available which is above 8 mm. With branching angle of 0.299° and device length of only 5 mm, the BPM simulation shows that the device could exhibits crosstalk of −33 dB at calculated required power of 26 mW.

Acknowledgements

The authors would like to thank the Ministry of Science, Technology and Innovation (MOSTI) for financing this project. Our gratitude also goes to the administration of Universiti Teknologi Malaysia (UTM) especially the Research Management Center (RMC) for their support and all members of Photonics Technology Centre.

References

[1] Silberberg Y, Perimutter P, Baran JE. Digital optical switch. Applied Physics Letter 1987;51:1230–2.
[2] Krahenbuhl R, Howerton MM, Dubinger J, Greenblatt AS. Performance and modeling of advanced Ti:LiNbO3. IEEE Journal of Lightwave Technology 2002;20:92–9.
[3] Noh Y-O, Lee C-H, Kim J-M, Hwang W-Y, Won Y-H, Lee H-J, Han S-G, Oh M-C. Polymer waveguide variable optical attenuator and its reliability. Optics Communications 2004;242:533–40.
[4] Supa'at ASM, Ibrahim MH, Mohammad AB, Kassim NM, Ghazali NE. A novel thermooptic polymer switch based on directional coupler structure. American Journal of Applied Sciences 2008;5:1552–7.
[5] Al-hetar AM, Yulianti I, Supa'at ASM, Mohammad AB. Thermo-optic multimode interference switches with air and silicon trenches. Optics Communications 2008;281:4653–7.
[6] Hoekstra HJWM. Optimisation of digital optical switches. Optical and Quantum Electronics 2000;32:843–54.
[7] Iodice M, Mazzi G, Sirleto L. Thermo-optical static and dynamic analysis of a digital optical switch based on amorphous silicon waveguide. Optics Express 2006;14:5266–78.
[8] Burns WK. Shaping the digital switch. IEEE Photonics Technology Letter 1992;4:861–3.
[9] Okayama H, Kawahara M. Reduction of voltage-length product for Y-branch digital optical switch. Journal of Lightwave Technology 1993;11:379–87.
[10] Yulianti I, Supa'at ASM, Idrus SM, Mohammad AB, Al-hetar AM, Beam propagation modelling of the digital response in cosine S-bend waveguide branch. In: Proceeding of international conference on semiconductor electronics 2008 (Malaysia, 2008).
[11] Moosburger R, Kostrzewa C, Fischbeck G, Petermann K. Shaping the digital optical switch using evolution strategies BPM. IEEE Photonics Technology Letters 1997;9:1484–6.
[12] Hauffe R, Integrated optical switching matrices constructed from digital optical switches based on polymeric rib waveguides. (PhD Dissertation, Technischen Universitat Berlin, 2002).
[13] Yulianti I, Supa'at ASM, Idrus SM, Cosine S-bend hybrid junction digital optical switch. In: Proceeding of international conference on photonics in switching 2008 (Hokkaido, Japan, 2008).
[14] Wang W-K, Lee HJ, Anthony PJ. Planar silica-glass optical waveguides with thermally induced lateral mode confinement. IEEE Journal of Lightwave Technology 1996;14:429–36.
[15] Majumdar P. Computational Methods for Heat and Mass Transfer. New York: Taylor & Francis Group; 2005.
[16] Van Krevelen DW. Properties of Polymers. Amsterdam: Elsevier; 1990.
[17] Lee S-S, Bu J-U, Lee S-Y, Song K-C, Park C– G, Kim T-S. Low-power consumption polymeric attenuator using a micromachined membrane-type waveguide. IEEE Photonics Technology Letters 2000;12:407–9.